

1 **Expression level of the reprogramming factor NeuroD1 is critical for neuronal**
2 **conversion efficiency from different cell types**

3
4 Kanae Matsuda-Ito^{1,2}, Taito Matsuda^{1,2*} and Kinichi Nakashima^{1*}

5
6 **Affiliations:**

7 1. Stem Cell Biology and Medicine, Department of Stem Cell Biology and Medicine,
8 Graduate School of Medical Sciences, Kyushu University, Fukuoka 812-8582, Japan

9 2. These authors contributed equally

10
11 * Correspondence:

12 Taito Matsuda,

13 Department of Stem Cell Biology and Medicine,

14 Graduate School of Medical Sciences, Kyushu University,

15 3-1-1, Maidashi, Higashi-ku, Fukuoka 812-8582, Japan.

16 Phone: +81-92-642-6196; E-mail: tmatsuda@scb.med.kyushu-u.ac.jp

17
18 Kinichi Nakashima,

19 Department of Stem Cell Biology and Medicine,

20 Graduate School of Medical Sciences, Kyushu University,

21 3-1-1, Maidashi, Higashi-ku, Fukuoka 812-8582, Japan.

22 Phone: +81-92-642-6195; E-mail: kin1@scb.med.kyushu-u.ac.jp

23
24 **Summary**

25 Several transcription factors, including NeuroD1, have been shown to act as neuronal
26 reprogramming factors (RFs) that induce neuronal conversion from somatic cells.

27 However, it remains unexplored whether expression levels of RFs in the original cells
28 affect reprogramming efficiency. Here, we show that the neuronal reprogramming

29 efficiency from two distinct glial cell types, microglia and astrocytes, is substantially
30 dependent on the expression level of NeuroD1: low expression failed to induce neuronal

31 reprogramming, whereas elevated NeuroD1 expression dramatically improved
32 reprogramming efficiency in both cell types. Moreover, even under conditions where

33 NeuroD1 expression was too low to induce effective conversion by itself, combined

34 expression of three RFs (Ascl1, Brn2, and NeuroD1) facilitated the breaking down of
35 cellular barriers, inducing neuronal reprogramming. Thus, our results suggest that a
36 sufficiently high expression level of RFs or alternatively their combinatorial expression,
37 is the key to achieving efficient neuronal reprogramming from different cells.

38

39 **Highlights**

- 40 ▪ High expression of NeuroD1 is required for neuronal conversion.
- 41 ▪ **Multiple infections with NeuroD1-expressing virus enhance neuronal**
42 **reprogramming**
- 43 ▪ **Combinatorial expression of NeuroD1 with other RFs facilitates neuronal**
44 **conversion**

45

46

47 **eTOC blurb**

48 In this article, Matsuda-Ito *et al.* demonstrate that the efficacy of conversion into neurons
49 from two distinct glial cells, microglia and astrocytes, depends on the NeuroD1
50 expression level. They also show that increased NeuroD1 expression alone enables
51 efficient neuronal reprogramming in non-reactive astrocytes that were previously shown
52 to be difficult to convert into neurons.

53

54

55 **Introduction**

56 Lineage-specific transcription factors induce direct reprogramming of somatic
57 cells to other cell types, such as neurons, without passing through a pluripotent stem cell
58 state. In 2010, mouse fibroblasts were shown to be directly converted to neurons *in vitro*
59 by forced expression of three transcription factors, Ascl1, Brn2, and Myt11 (Vierbuchen
60 *et al.*, 2010). More recently, by examining combinations of factors used for
61 reprogramming, it has become possible to convert fibroblasts to neurons of specific
62 subtypes, such as sensory and motor neurons (Masserdotti *et al.*, 2016; Matsuda and
63 Nakashima, 2021). Several groups have reported *in vivo* neuronal reprogramming into
64 neurons from glial cells, including astrocytes, which become reactive after brain damage
65 and eventually contribute to glial scar formation. For example, ectopic expression of Sox2,
66 Neurog2, or NeuroD1 converts endogenous astrocytes to neurons in the mouse brain (Guo

67 et al., 2014; Mattugini et al., 2019; Niu et al., 2013; Wu et al., 2020). Microglia, a type of
68 glial cell, are the resident immune cells in the brain and are derived from primitive
69 macrophages (Ginhoux et al., 2010). Microglia accumulate at the injured site to remove
70 dead cells after brain injury, such as stroke, and consequently become the predominant
71 cell type in the ischemic core region (Annunziato et al., 2013). We have previously shown
72 that microglia can be converted into neurons both *in vitro* and *in vivo* by the ectopic
73 expression of lentivirus-encoded NeuroD1 (Matsuda et al., 2019). Although *in vivo*
74 neuronal reprogramming from these two glial cells holds great promise as a therapeutic
75 strategy, further improvement of neuronal reprogramming efficiency is warranted to
76 supply sufficient numbers of new neurons for complete functional recovery from
77 neurological injury and diseases.

78 In a previous report, single-cell RNA sequencing analysis indicated that high
79 but not low expression of *Ascl1* induced the expression of neuronal marker genes in
80 fibroblasts (Treutlein et al., 2016), implying a correlation between transgene expression
81 level and the attainment of neuronal reprogramming. However, it has not been extensively
82 studied how the conditions in which reprogramming factors (RFs) are expressed influence
83 neuronal reprogramming efficiency. Here, we examined neuronal reprogramming from
84 microglia and astrocytes under conditions of different expression levels of NeuroD1 in
85 these two glial cell types. In contrast to the higher expression, when we decreased the
86 expression of NeuroD1 by reducing doxycycline (Dox) concentration, the neuronal
87 conversion from microglia was dramatically diminished. On the other hand, increasing
88 the NeuroD1 expression level by repeated lentiviral infections (2 times) improved
89 neuronal reprogramming efficiency from microglia. Moreover, multiple NeuroD1-
90 expressing viral infections (3 times) enabled neuronal reprogramming from non-reactive
91 (NR-) astrocytes that were previously shown to be difficult to convert into neurons with
92 a single infection (Matsuda et al., 2019). We also found that the combined expression of
93 three RFs, *Ascl1* and *Brn2* together with NeuroD1, efficiently induced neuronal
94 reprogramming, even when their expression was low. Taking these observations together,
95 we believe that our study offers efficient strategies to reprogram neurons from glial cells
96 and will contribute to accelerating the development of therapeutic applications for brain
97 injury and diseases.

98

99

100 **Results**

101 **NeuroD1 expression level-dependent changes in reprogramming efficiency**

102 To investigate whether the efficiency of microglia-to-neuron (MtN)
103 reprogramming is influenced by the expression level of NeuroD1, we used a lentivirus
104 expressing NeuroD1 under the control of the Dox-inducible tetracycline response element
105 promoter. We isolated CD68-, Iba1-, and Tmem119-positive (CD68⁺ Iba1⁺ Tmem119⁺)
106 microglia from the 1-day-old mouse cortex with the same high purity as in our previous
107 study (Matsuda et al., 2019) (Figure 1A) and added an equal amount of virus to each
108 microglial culture dish, but treated them with different doses of Dox. At 7 days post
109 treatment (dpt), we observed the Dox-dose dependent appearance of EGFP⁺ cells (Figures
110 1B and 1C). We next examined MtN conversion efficiency in the individual dishes based
111 on the proportion of β III-tubulin⁺/EGFP⁺ cells among Hoechst⁺ total cells and found that
112 the efficiency was greatly decreased by reducing the Dox concentration (Figure 1D).
113 Consistent with this, although no further increase of *NeuroD1* expression was observed
114 at 2 μ g/mL of Dox compared to 1 μ g/mL (Figure 1E), the *NeuroD1* expression decreased
115 in a Dox concentration-dependent manner (Figure 1E), suggesting that a low level of
116 NeuroD1 expression cannot effectively induce MtN conversion but that NeuroD1 *per se*
117 is able to do so if highly expressed. To compare the protein expression levels of NeuroD1
118 per cell under different Dox concentrations, microglia were transduced with FLAG-
119 tagged NeuroD1 and treated with Dox at 1 μ g/mL or 0.01 μ g/mL. We observed reduced
120 protein expression of both NeuroD1 and EGFP at single-cell resolution at the lower dose
121 relative to the higher one (Figure 1F). These data indicate that NeuroD1 expression above
122 a certain threshold level is required for the effective induction of MtN conversion.

123

124 **Elevated expression level of NeuroD1 enhances neuronal reprogramming**

125 We next explored whether increasing the expression level of NeuroD1
126 promotes neuronal reprogramming from astrocytes in addition to microglia. We prepared
127 mouse NR-astrocytes *in vitro*, treated them with AraC, and allowed them to grow without
128 growth factors: these astrocytes have a state closely resembling that of astrocytes under
129 the physiological conditions (Figure 2A) (Laywell et al., 2000; White et al., 2011). GFAP-
130 expressing NR-astrocytes were transduced with FLAG-NeuroD1 and EGFP by single
131 (\times 1) or repeated (\times 3) viral infections, and we found that the repeated infection increased

132 both NeuroD1 and EGFP protein expression levels at the single-cell level (Figures 2B
133 and 2C). When we checked reprogramming efficiency, single NeuroD1 lentivirus
134 infection hardly induced neuronal reprogramming from NR-astrocytes in agreement with
135 our previous reports (Brulet et al., 2017; Matsuda et al., 2019), whereas elevated
136 expression of NeuroD1 by repeated infections dramatically promoted astrocyte-to-neuron
137 (AtN) conversion at 7 dpt (Figures 2D and 2E). Repeated viral infection ($\times 2$) also
138 increased MtN reprogramming efficiency (Figures 2F and 2G). These data indicate that
139 increased NeuroD1 expression enables efficient neuronal reprogramming even from cells
140 that are difficult to convert.

141

142 **Differences in cell context affect neuronal reprogramming efficiency**

143 In contrast to our study, astrocytes were previously cultured in the presence of
144 growth factors, FGF2 and EGF (Guo et al., 2014; Heinrich et al., 2010), both of which
145 are expressed in reactive astrocytes and allow the response to signaling pathways critical
146 to neuronal fate choice (Buffo et al., 2008; Burda and Sofroniew, 2014; Robel et al., 2011).
147 To ask whether fundamental environmental differences affect neuronal reprogramming
148 efficiency, we isolated astrocytes and cultured them in the continuous presence of FGF2
149 and EGF. By this growth factor treatment alone, a small percentage of β III-tubulin⁺ cells
150 among control virus-infected cells appeared (Figures 3A and 3C), probably because
151 FGF2 and EGF can confer stem cell-like properties on astrocytes, enabling them to
152 differentiate into neurons in accordance with previous reports (Kleiderman et al., 2016;
153 Magnusson et al., 2020). In addition, unlike in the absence of these growth factors
154 (Figures 2C and 2D), we found that even a single NeuroD1 virus infection together with
155 FGF2 and EGF could effectively induce AtN conversion by 7 dpt (Figures 3B and 3C).
156 We then assessed whether subsequent FGF2 and EGF stimulation affect neuronal
157 reprogramming from NR-astrocytes established in the absence of the growth factors.
158 After 3 days' stimulation with FGF2 and EGF, NeuroD1 expression was induced with 1
159 μ g/ml of Dox in NR-astrocytes infected only once with NeuroD1 lentivirus. We found
160 that FGF2 and EGF stimulation allowed NR-astrocytes exposed to a single NeuroD1
161 virus infection to be converted into neurons (Figures 3D and 3E). In addition to FGF2
162 and EGF, LIF is expressed in reactive astrocytes and is known to affect their properties
163 (Linnerbauer and Rothhammer, 2020). However, LIF stimulation did not improve the
164 neuronal conversion efficiency of NR-astrocytes. Thus, these results indicate that

165 environmental factors, especially those that confer stem cell-like properties on astrocytes,
166 can contribute to efficient AtN conversion.

167

168 **Combinatorial expression of RFs enhances neuronal reprogramming**

169 Besides increasing the expression level of RFs and environmental factors,
170 combinatorial expression of RFs is another strategy that should be considered to enhance
171 neuronal reprogramming efficiency (Matsuda and Nakashima, 2021). The neurogenic
172 transcription factors *Ascl1* and *Brn2* have been shown to induce neuronal reprogramming
173 from somatic cells, including astrocytes and microglia (Gascón et al., 2016; Matsuda et
174 al., 2019). Therefore, we first expressed *Ascl1* and *Brn2* together with *NeuroD1* (NAB)
175 in microglia and found that this NAB combination augmented MtN conversion compared
176 to *NeuroD1* alone even with a low dose (0.1 µg/mL) of Dox (Figures 4A and 4B). We
177 further observed that the efficiency of AtN conversion was dramatically increased by Dox
178 (1 µg/mL)-induced NAB expression compared to *NeuroD1* expression alone, in which
179 AtN conversion was negligible (Figures 4C and 4D). These results indicate that
180 reprogramming efficiency can be positively modulated by combining optimal RFs even
181 under conditions where reprogramming occurs inefficiently.

182

183 **Discussion**

184 In this study, using *NeuroD1* as a representative RF, we have shown that
185 reprogramming efficiency is influenced by the three factors: RF expression level,
186 environmental factors, and the combination of RFs. In addition, we demonstrated that if
187 the RF expression is sufficiently high, neurons can be induced with a single RF even in
188 cells that are difficult to reprogram. In other words, this finding suggests that the key
189 determinant of successful neuronal reprogramming among the three factors is the RF
190 expression level.

191 We have previously revealed that in microglia, ectopically expressed *NeuroD1*
192 binds to closed chromatin with bivalent modifications, namely active (trimethylation of
193 histone H3 at lysine 4 [H3K4me3]) and repressive (H3K27me3) marks, to induce the
194 expression of neuronal genes (Matsuda et al., 2019). In contrast to microglia, NR-
195 astrocytes lack such bivalent signatures and exhibit a monovalent repressive modification
196 (H3K27me3) around neuronal gene loci, in accordance with the low capacity of *NeuroD1*
197 to induce neuronal conversion of these cells (Matsuda et al., 2019). However, another

198 study demonstrated that NeuroD1 could occupy loci possessing the H3K27me3
199 modification to initiate neuronal programs in ES cells (Pataskar et al., 2016). In the
200 present study, we found that a relatively higher expression level of NeuroD1 induced by
201 repeated virus infections could achieve neuronal reprogramming efficiently from NR-
202 astrocytes. These findings suggest that while NeuroD1 preferentially binds to regions
203 with bivalent modifications, an excess amount of NeuroD1 may increase the likelihood
204 that it will also bind to regions with a monovalent repressive modification to initiate the
205 neuronal program.

206 Recent studies have shown that the AtN conversion efficiency differs
207 depending on the brain region in which the astrocytes reside. For example, astrocytes in
208 the corpus callosum cannot be reprogrammed into neurons by expression of either
209 NeuroD1 or the combination of Neurog2 and Nurr1, whereas astrocytes in the cortex can
210 be (Liu et al., 2020; Mattugini et al., 2019), implying that the particular environment in
211 different brain regions dictates distinct astrocytic properties and consequently affects
212 reprogramming potential. Astrocytes have been reported to acquire a variety of
213 phenotypes and gene expression patterns in response to many pathological stimuli, such
214 as stroke, neurodegenerative diseases, and aging (Matias et al., 2019). We found in the
215 present study that FGF2- and EGF-stimulated astrocytes are more likely to be converted
216 into neurons than LIF-stimulated astrocytes, although all three of these factors are
217 expressed and regulate the behavior of reactive astrocytes in pathological conditions
218 (Linnerbauer and Rothhammer, 2020). This result indicates that reprogramming
219 efficiency from astrocytes may vary depending on brain pathologies as well as brain
220 regions. Moreover, microglia have also recently been shown to manifest phenotypic
221 heterogeneity across different regions and under neurological diseases in the brain
222 (Deczkowska et al., 2018; Tan et al., 2020). Therefore, it is critical that neuronal
223 reprogramming should be achieved by ensuring sufficient expression of RFs and, if
224 necessary, examining their combinations to apply this technology to brain injury and
225 disease therapy.

226 Our findings provide insights into how RF expression levels affect neuronal
227 reprogramming efficiency and ways to efficiently induce neurons from two glial cell
228 types, microglia and astrocytes. Boosting reprogramming efficiency should offer
229 therapeutic strategies for neurological conditions such as Alzheimer's disease, spinal cord
230 injury and ischemia.

231

232 **Experimental procedures**

233 **Isolation and culture of primary microglia and astrocytes**

234 We prepared primary microglia and astrocytes from mouse at postnatal day 1 using a
235 previously reported protocol (Matsuda et al., 2019), with some modifications. We
236 dissected cortexes of ICR mice after peeling of meninges to obtain microglia and
237 astrocytes from glial cell mixtures. Dissected tissues were digested with papain (22.5U/ml,
238 Sigma) at 37°C for 30 min and treated with DNase (200U/ml, Sigma). After
239 centrifugation (200 × g, 5 min), the cell pellet was suspended in alpha minimum essential
240 medium (MEM) with 5% fetal bovine serum (FBS) and 0.6% glucose and filtered with a
241 40-µm cell strainer (BD Falcon). After centrifugation (200 × g, 5 min), the cell pellet was
242 again suspended in alpha MEM and re-centrifuged (200 × g, 5 min). The cell pellets were
243 resuspended in Dulbecco's modified Eagle's medium (DMEM)/Ham's F-12 (Nacalai
244 Tesque) containing 20% FBS, 1 mM L-sodium pyruvate, and MEM nonessential amino
245 acids solution, and treated with GM-CSF (2.5 ng/mL; R&D Systems) to enhance
246 microglial proliferation. This isolated glial mixture was plated in T75 tissue culture flasks
247 (BD Falcon) and the medium was changed every 2–3 days. Subsequently, we collected
248 microglia by strong shaking for 1 h after 7–10 days in culture. The microglia were then
249 plated onto an uncoated 35-mm culture dish and oligodendrocytes were removed by
250 changing the medium 30 min after plating. We used the cells attached to the dish as
251 primary cultured microglia and maintained them in DMEM/Ham's F-12 containing 20%
252 FBS, 1 mM L-sodium pyruvate, and MEM nonessential amino acids solution.

253 After isolation of microglia, flasks were treated with AraC (5 µM) for 2 days
254 to remove proliferating cells. Cultures were shaken for 16 h, and then trypsin–EDTA
255 solution was added to the flask to obtain NR-astrocytes. Isolated NR-astrocytes were
256 plated onto an uncoated 35-mm culture dish and maintained with DMEM/Ham's F-12
257 containing 20% FBS.

258 To isolate FGF2- and EGF-stimulated astrocytes, the cell pellet obtained from
259 dissected cortical tissues was cultured in T75 tissue culture flasks using DMEM/Ham's
260 F-12 containing 20% FBS, hEGF (10 ng/mL, Peprotech), hFGF2 (10 ng/mL, Peprotech),
261 and B27. The medium was changed every 2 days. After 5–7 days of culture, trypsin–
262 EDTA solution was added to the flask and the isolated cells were plated onto an uncoated

263 35-mm culture dish. FGF2 and EGF (10 ng/mL) or 50 ng/mL LIF were used to stimulate
264 NR-astrocytes.

265

266 **Virus production**

267 Lentiviruses were produced by transfecting HEK293T cells in a 10-cm dish with the
268 constructs pCMV-VSV-G-RSV-Rev and pCAG-HIVgp using polyethylenimine. Since
269 lot-to-lot variation in FBS preparations added to the culture medium critically influences
270 the resultant viral tropism, we avoided using FBS for virus preparation (Torashima et al.,
271 2007). After transfection, we cultured the cells with 5 mL of serum-free N2 medium
272 (DMEM/F12 supplemented with insulin (25 µg/mL), apo-transferrin (100 µg/mL),
273 progesterone (20 nM), putrescine (60 µM), and sodium selenite (30 nM)) for 2 days. The
274 supernatant was collected and used for virus infection experiments after filtration through
275 a 0.2 filter to remove cell debris.

276

277 **Induction of neuronal conversion**

278 To induce neurons from glial cells, we used lentiviral vectors (derived from the Tet-O-
279 FUW vector) in which gene expression is controlled by the tetracycline operator.
280 Plasmids used in this study are similar to those described in our previous report (Matsuda
281 et al., 2019). For cells to be infected efficiently with the lentivirus, the virus must be added
282 as soon as possible after plating the microglia. Therefore, virus suspensions were added
283 at the time of medium exchange 30 min after isolation of primary microglia, and infection
284 was performed overnight. The medium was then replaced with a neuronal medium
285 (Neurobasal Medium (GIBCO) supplemented with B27 (Gibco), GlutaMAX (2 mM,
286 Gibco), BDNF, GDNF, NT3 (10 ng/mL each, Peprtech), and
287 penicillin/streptomycin/fungizone (Hyclone), and Dox induction was started for 7 days
288 to convert microglia into neuronal cells. Dox was added only once to the medium to
289 activate RF expression. The medium was changed every 2–3 days for the duration of the
290 culture period.

291 For conversion into neuronal cells from astrocytes, the virus suspension was
292 added at the time the cells were seeded, and infection was performed overnight. The
293 medium was replaced with neuronal medium the next day, and Dox induction was started
294 for 7 days to convert astrocytes into neuronal cells.

295 For sequential viral infections, a second infection was performed 8 h after the
296 first infection was completed, and overnight virus infection and medium replacement
297 were repeated. To convert glial cells into neuronal cells, the medium was replaced with
298 neuronal medium containing Dox after the final infection and the cells were cultured for
299 7 days. The medium was changed every 2–3 days for the duration of the culture period.

300

301 **Immunocytochemistry**

302 Cells were fixed in 4% paraformaldehyde for 10 min and blocked for 1 h at room
303 temperature (RT) with blocking buffer (5% FBS and 0.3% Triton X-100). After blocking,
304 the cells were incubated with the following primary antibodies for 2 h at RT: anti- β III-
305 tubulin (1:500, Covance), anti-Map2ab (1:500, Sigma), anti-GFP (1:500, Aves), anti-
306 FLAG (1:500, Sigma), anti-Tmem119 (1:500, Abcam), anti-CD68 (1:500, Bio-Rad), and
307 anti-Iba1 (1:500, Abcam). Stained cells were visualized with a fluorescence microscope
308 (Axiovert 200M, Zeiss) and a confocal microscope (LSM800, Zeiss). Fluorescence
309 intensity of the cell soma was quantified using LAS AF (Leica) or ZEN (Zeiss).

310

311 **Real-time qRT-PCR**

312 Total RNA was isolated using an RNeasy Micro Kit (QIAGEN) according to the
313 supplier's protocol. RNA quality was checked with a spectrophotometer. Reverse
314 transcription reactions were performed using a SuperScript VILO cDNA Synthesis Kit
315 (Life Technologies) following the supplier's protocol. qRT-PCR was performed with
316 SYBR green fluorescent dye using Step One Plus (Applied Biosystems) and Mx3000
317 (Stratagene). GAPDH was used as an endogenous control to normalize samples. The PCR
318 primers used in this study were

319 NeuroD1_Fw:AAGCCACGGATCAATCTTCTC and

320 NeuroD1_Rv:CGTGAAAGATGGCATTAAAGCTG.

321

322 **Statistical analysis**

323 Data were analyzed using Prism 9 ver.9.1.2. Unpaired Student's t tests were used to
324 calculate the p value for pairwise comparisons. For multiple comparisons, p values were
325 calculated using one-way ANOVA with the Tukey *post hoc* test. Data represent mean \pm
326 SEM. We considered probabilities of $p < 0.05$ to be significant.

327

328 **Author contributions**

329 K.M-I., T.M., and K.N. designed research and analyzed data; K.M-I. and T.M. performed
330 research; K.M-I., T.M., and K.N. wrote the paper.

331

332 **Acknowledgments**

333 We thank Y. Nakagawa for excellent secretarial assistance and I. Smith for proofreading
334 the manuscript. This work was supported by a Grant-in-Aid for Research Activity Start-
335 up JP21K20639 (to K.M-I.), a Grant-in-Aid for Scientific Research (B) JP21H02808 (to
336 T.M.), the Takeda Science Foundation (to T.M.), a research grant from the Noguchi
337 Institute (to T.M.), AMED JP21bm0404057 (to T.M., K.N.), and a Grant-in-Aid for
338 Scientific Research on Innovative Areas 17 JP16K21734 (to K.N.).

339

340 **Conflicts of interest**

341 The authors declare no competing interests.

342

343 **References**

344 Annunziato, L., Boscia, F., and Pignataro, G. (2013). Ionic Transporter Activity in
345 Astrocytes, Microglia, and Oligodendrocytes During Brain Ischemia. *Journal of Cerebral*
346 *Blood Flow & Metabolism* 33.

347 Brulet, R., Matsuda, T., Zhang, L., Miranda, C., Giacca, M., Kaspar, B.K., Nakashima,
348 K., and Hsieh, J. (2017). NEUROD1 Instructs Neuronal Conversion in Non-Reactive
349 Astrocytes. *Stem Cell Reports* 8.

350 Buffo, A., Rite, I., Tripathi, P., Lepier, A., Colak, D., Horn, A.-P., Mori, T., and Gotz, M.
351 (2008). Origin and progeny of reactive gliosis: A source of multipotent cells in the injured
352 brain. *Proceedings of the National Academy of Sciences* 105.

353 Burda, J.E., and Sofroniew, M.V. (2014). Reactive Gliosis and the Multicellular
354 Response to CNS Damage and Disease. *Neuron* 81.

355 Deczkowska, A., Keren-Shaul, H., Weiner, A., Colonna, M., Schwartz, M., and Amit, I.
356 (2018). Disease-Associated Microglia: A Universal Immune Sensor of
357 Neurodegeneration. *Cell* 173.

358 Gascón, S., Murenu, E., Masserdotti, G., Ortega, F., Russo, G.L., Petrik, D., Deshpande,
359 A., Heinrich, C., Karow, M., Robertson, S.P., et al. (2016). Identification and Successful

360 Negotiation of a Metabolic Checkpoint in Direct Neuronal Reprogramming. *Cell Stem*
361 *Cell* 18.

362 Ginhoux, F., Greter, M., Leboeuf, M., Nandi, S., See, P., Gokhan, S., Mehler, M.F.,
363 Conway, S.J., Ng, L.G., Stanley, E.R., et al. (2010). Fate Mapping Analysis Reveals That
364 Adult Microglia Derive from Primitive Macrophages. *Science* 330.

365 Guo, Z., Zhang, L., Wu, Z., Chen, Y., Wang, F., and Chen, G. (2014). In Vivo Direct
366 Reprogramming of Reactive Glial Cells into Functional Neurons after Brain Injury and
367 in an Alzheimer's Disease Model. *Cell Stem Cell* 14.

368 Heinrich, C., Blum, R., Gascón, S., Masserdotti, G., Tripathi, P., Sánchez, R., Tiedt, S.,
369 Schroeder, T., Götz, M., and Berninger, B. (2010). Directing Astroglia from the Cerebral
370 Cortex into Subtype Specific Functional Neurons. *PLoS Biology* 8.

371 Kleiderman, S., Gutbier, S., Ugur Tufekci, K., Ortega, F., Sá, J. v., Teixeira, A.P., Brito,
372 C., Glaab, E., Berninger, B., Alves, P.M., et al. (2016). Conversion of Nonproliferating
373 Astrocytes into Neurogenic Neural Stem Cells: Control by FGF2 and Interferon- γ . *STEM*
374 *CELLS* 34.

375 Laywell, E.D., Rakic, P., Kukekov, V.G., Holland, E.C., and Steindler, D.A. (2000).
376 Identification of a multipotent astrocytic stem cell in the immature and adult mouse brain.
377 *Proceedings of the National Academy of Sciences* 97.

378 Linnerbauer, M., and Rothhammer, V. (2020). Protective Functions of Reactive
379 Astrocytes Following Central Nervous System Insult. *Frontiers in Immunology* 11.

380 Liu, M.-H., Li, W., Zheng, J.-J., Xu, Y.-G., He, Q., and Chen, G. (2020). Differential
381 neuronal reprogramming induced by NeuroD1 from astrocytes in grey matter versus
382 white matter. *Neural Regeneration Research* 15.

383 Magnusson, J.P., Zamboni, M., Santopolo, G., Mold, J.E., Barrientos-Somarribas, M.,
384 Talavera-Lopez, C., Andersson, B., and Frisén, J. (2020). Activation of a neural stem cell
385 transcriptional program in parenchymal astrocytes. *ELife* 9.

386 Masserdotti, G., Gascón, S., and Götz, M. (2016). Direct neuronal reprogramming:
387 learning from and for development. *Development* 143.

388 Matias, I., Morgado, J., and Gomes, F.C.A. (2019). Astrocyte Heterogeneity: Impact to
389 Brain Aging and Disease. *Frontiers in Aging Neuroscience* 11.

390 Matsuda, T., and Nakashima, K. (2021). Natural and forced neurogenesis in the adult
391 brain: Mechanisms and their possible application to treat neurological disorders.
392 *Neuroscience Research* 166.

393 Matsuda, T., Irie, T., Katsurabayashi, S., Hayashi, Y., Nagai, T., Hamazaki, N., Adefuin,
394 A.M.D., Miura, F., Ito, T., Kimura, H., et al. (2019). Pioneer Factor NeuroD1 Rearranges
395 Transcriptional and Epigenetic Profiles to Execute Microglia-Neuron Conversion.
396 *Neuron* 101.

397 Mattugini, N., Bocchi, R., Scheuss, V., Russo, G.L., Torper, O., Lao, C.L., and Götz, M.
398 (2019). Inducing Different Neuronal Subtypes from Astrocytes in the Injured Mouse
399 Cerebral Cortex. *Neuron* 103.

400 Niu, W., Zang, T., Zou, Y., Fang, S., Smith, D.K., Bachoo, R., and Zhang, C.-L. (2013).
401 In vivo reprogramming of astrocytes to neuroblasts in the adult brain. *Nature Cell Biology*
402 15.

403 Pataskar, A., Jung, J., Smialowski, P., Noack, F., Calegari, F., Straub, T., and Tiwari, V.K.
404 (2016). NeuroD1 reprograms chromatin and transcription factor landscapes to induce the
405 neuronal program. *The EMBO Journal* 35.

406 Robel, S., Berninger, B., and Götz, M. (2011). The stem cell potential of glia: lessons
407 from reactive gliosis. *Nature Reviews Neuroscience* 12.

408 Tan, Y.-L., Yuan, Y., and Tian, L. (2020). Microglial regional heterogeneity and its role
409 in the brain. *Molecular Psychiatry* 25.

410 Torashima, T., Koyama, C., Higashida, H., and Hirai, H. (2007). Production of neuron-
411 preferential lentiviral vectors. *Protocol Exchange*.

412 Treutlein, B., Lee, Q.Y., Camp, J.G., Mall, M., Koh, W., Shariati, S.A.M., Sim, S., Neff,
413 N.F., Skotheim, J.M., Wernig, M., et al. (2016). Dissecting direct reprogramming from
414 fibroblast to neuron using single-cell RNA-seq. *Nature* 534.

415 Vierbuchen, T., Ostermeier, A., Pang, Z.P., Kokubu, Y., Südhof, T.C., and Wernig, M.
416 (2010). Direct conversion of fibroblasts to functional neurons by defined factors. *Nature*
417 463.

418 White, R.E., Rao, M., Gensel, J.C., McTigue, D.M., Kaspar, B.K., and Jakeman, L.B.
419 (2011). Transforming Growth Factor Transforms Astrocytes to a Growth-Supportive
420 Phenotype after Spinal Cord Injury. *Journal of Neuroscience* 31.

421 Wu, Z., Parry, M., Hou, X.-Y., Liu, M.-H., Wang, H., Cain, R., Pei, Z.-F., Chen, Y.-C.,
422 Guo, Z.-Y., Abhijeet, S., et al. (2020). Gene therapy conversion of striatal astrocytes into
423 GABAergic neurons in mouse models of Huntington's disease. *Nature Communications*
424 11.

425

426

427

428 **Figure legends**

429 **Figure 1 RF expression threshold is required to convert microglia efficiently into** 430 **neurons**

431 (A) Representative images of staining for microglial markers Tmem119 (green), CD68
432 (magenta), and Iba1 (cyan) in primary isolated microglia. Scale bar, 75 μ m. (B)
433 Representative images of staining for EGFP (green), and the neuronal markers β III-
434 tubulin (red) and Map2ab (cyan), in NeuroD1-transduced microglia at 7 dpt under the
435 indicated Dox concentration treatment conditions. Scale bars, 50 μ m. (C) Quantification
436 of the EGFP⁺ cells in (B) (n = 3). (D) Quantification of the β III-tubulin⁺ EGFP⁺ cells in
437 (B) (n = 3). (E) qRT-PCR analysis of total *NeuroD1* mRNA levels in NeuroD1-
438 transduced microglia at 2 dpt under the indicated Dox concentration treatment conditions
439 (n = 3 biological replicates). **p < 0.005, ****p < 0.0001 by ANOVA with Tukey *post hoc*
440 tests. (F) Representative images of staining for EGFP (green) and FLAG (red) in FLAG-
441 NeuroD1-transduced microglia at 2 dpt under 1 μ g/mL and 0.01 μ g/mL Dox induction
442 (left). Intensity of EGFP or FLAG in left panel (right). ****p < 0.0001 by unpaired
443 Student's t test. ns means not significant (P > 0.05).

444

445 **Figure 2 Conversion efficiency is promoted with increased RF expression level**

446 (A) Representative images of non-reactive astrocytes (NR-astrocytes) stained for the
447 astrocyte marker GFAP (red). Scale bar, 75 μ m. (B) Representative images of staining
448 for EGFP (green) and FLAG (red) in FLAG-NeuroD1-transduced NR-astrocytes at 2 dpt.
449 Dox, 1 μ g/mL. Scale bar, 100 μ m. (C) Fluorescence intensity of EGFP or FLAG in (B).
450 ****p < 0.0001 by unpaired Student's t test. (D) Representative images of staining for
451 EGFP (green), β III-tubulin (red), and Map2ab (cyan) in reprogrammed neuronal cells
452 from NR-astrocytes at 7dpt. Dox, 1 μ g/mL of Dox. Scale bars, 100 μ m. (E) Quantification
453 of the β III-tubulin and EGFP⁺ cells in (D) (n = 3). ****p < 0.0001 by unpaired Student's t
454 test. (F) Representative images of staining for EGFP (green), β III-tubulin (red), and
455 Map2ab (cyan) in reprogrammed neuronal cells from microglia at 7 dpt. Dox, 1 μ g/mL.
456 Scale bars, 100 μ m. (G) Quantification of the β III-tubulin and EGFP⁺ cells in (F) (n = 3).
457 ***p < 0.0005 by unpaired Student's t test.

458

459 **Figure 3 Environmental stimulation affects neuronal reprogramming efficiency**

460 (A) Representative images of staining for EGFP (green), β III-tubulin (red), and Map2ab
461 (cyan) in EGFP-transduced astrocytes cultured with EGF and FGF2 at 7 dpt. Dox, 1
462 $\mu\text{g/mL}$. Scale bar, 100 μm . (B) Representative images of staining for EGFP (green), β III-
463 tubulin (red), and Map2ab (cyan) in NeuroD1-transduced astrocytes cultured with EGF
464 and FGF2 at 7 dpt. Dox, 1 $\mu\text{g/mL}$. Scale bar, 100 μm . (C) Quantification of the β III-
465 tubulin and EGFP⁺ cells in (A and B) (n = 3). *p < 0.05 by unpaired Student's t test. (D)
466 Representative images of staining for EGFP (green), β III-tubulin (red), and Map2ab
467 (cyan) in NeuroD1-transduced NR-astrocytes cultured with EGF and FGF2, LIF, and
468 without these factors (Ctrl) at 7 dpt. EGF and FGF2 or LIF were applied for 3 days. Dox,
469 1 $\mu\text{g/mL}$. Scale bars, 100 μm . (E) Quantification of the β III-tubulin and EGFP⁺ cells in
470 (D) (n = 3). **p < 0.005 by ANOVA with Tukey *post hoc* tests. ns means not significant
471 (P > 0.05).

472

473 **Figure 4 Optimal combinations of RFs increase neuronal reprogramming efficiency**

474 (A) Representative images of staining for EGFP (green), β III-tubulin (red), and Map2ab
475 (cyan) in NeuroD1- or NAB-transduced microglia at 7 dpt. Dox, 0.1 $\mu\text{g/mL}$. Scale bars,
476 100 μm . (B) Quantification of the β III-tubulin and EGFP⁺ cells in (A) (n = 3). *p < 0.05
477 by unpaired Student's t test. (C) Representative images of staining for EGFP (green), β III-
478 tubulin (red), and Map2ab (cyan) in NeuroD1- or NAB-transduced NR-astrocytes at 7
479 dpt. Dox, 1 $\mu\text{g/mL}$. Scale bars, 100 μm . (D) Quantification of the β III-tubulin and EGFP
480 ⁺ cells in (C) (n = 3). ***p < 0.0005 by unpaired Student's t test.

481

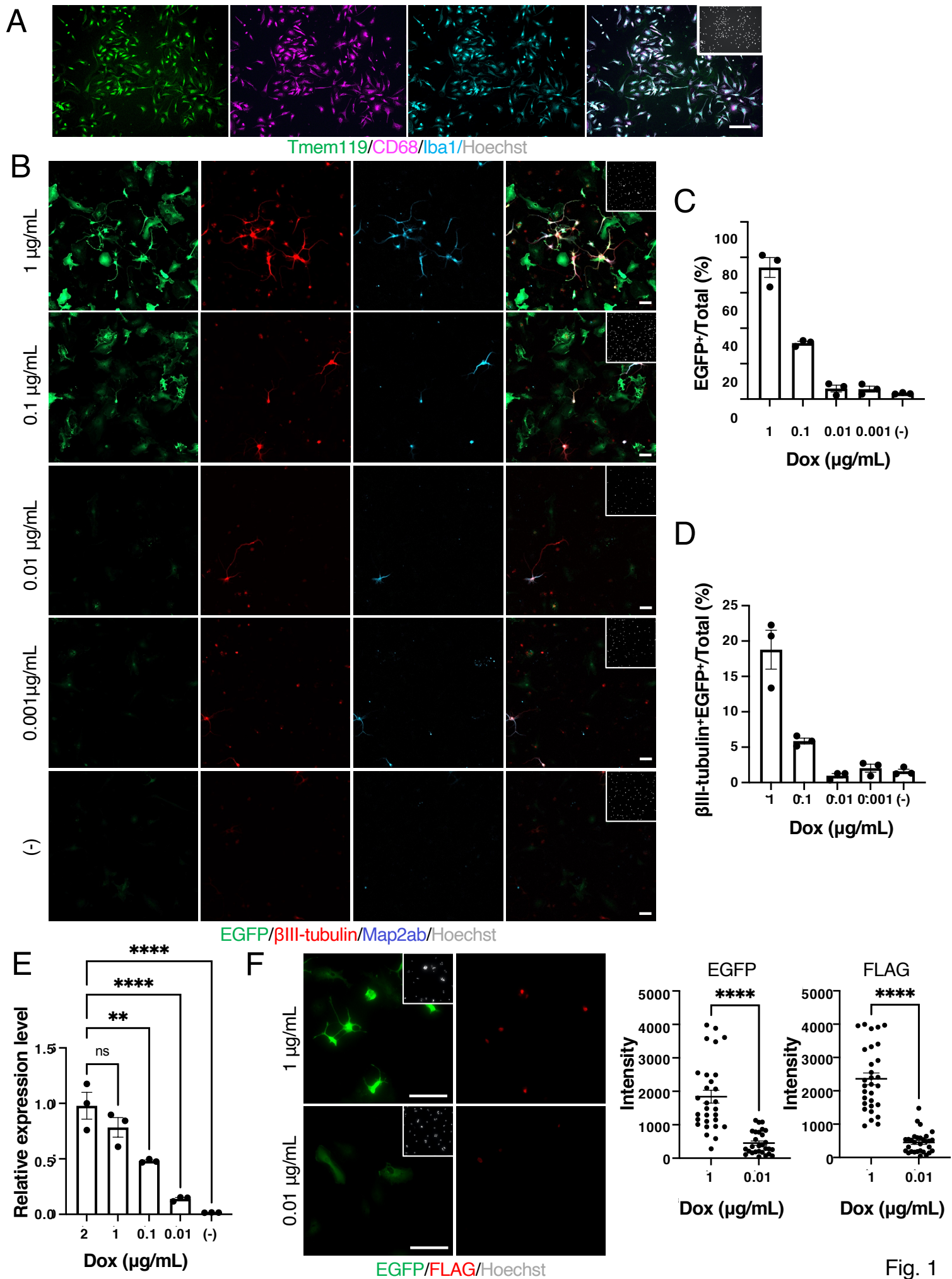


Fig. 1

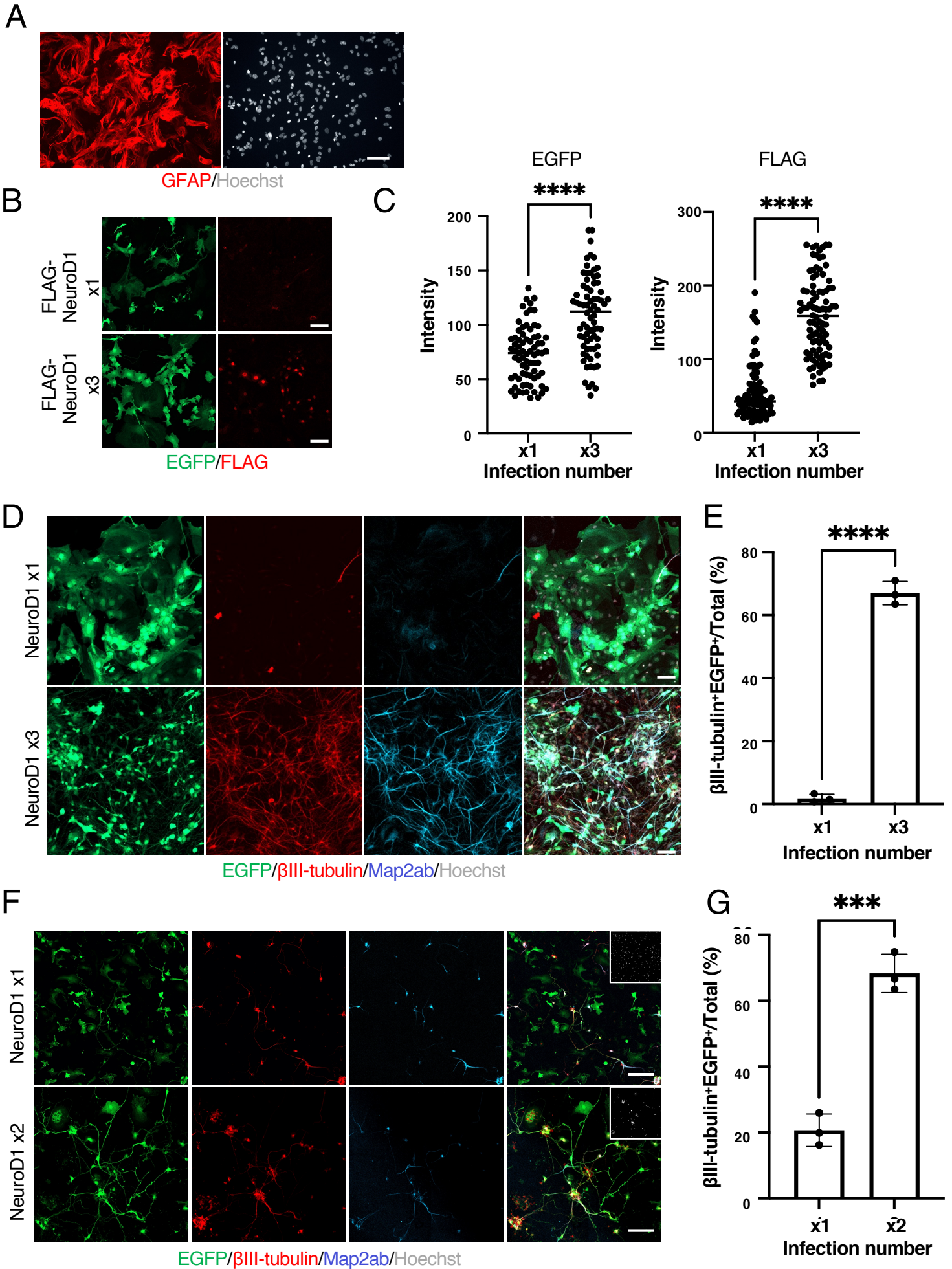


Fig. 2

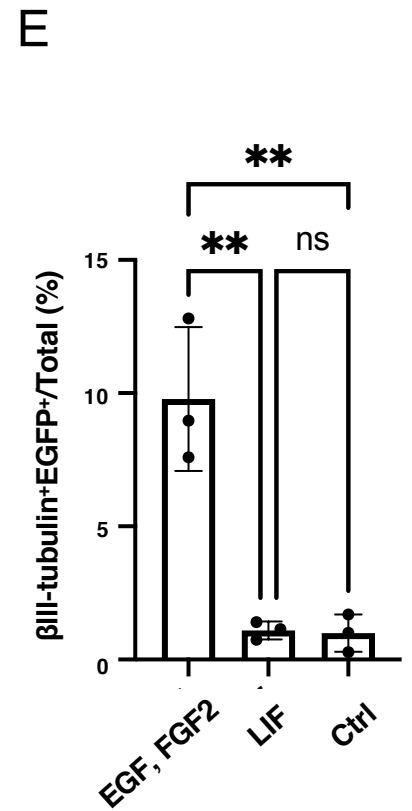
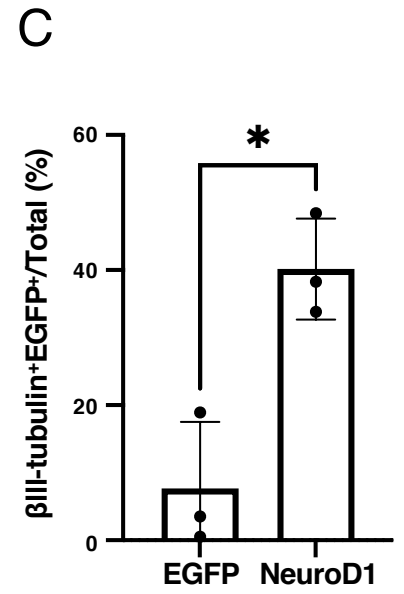
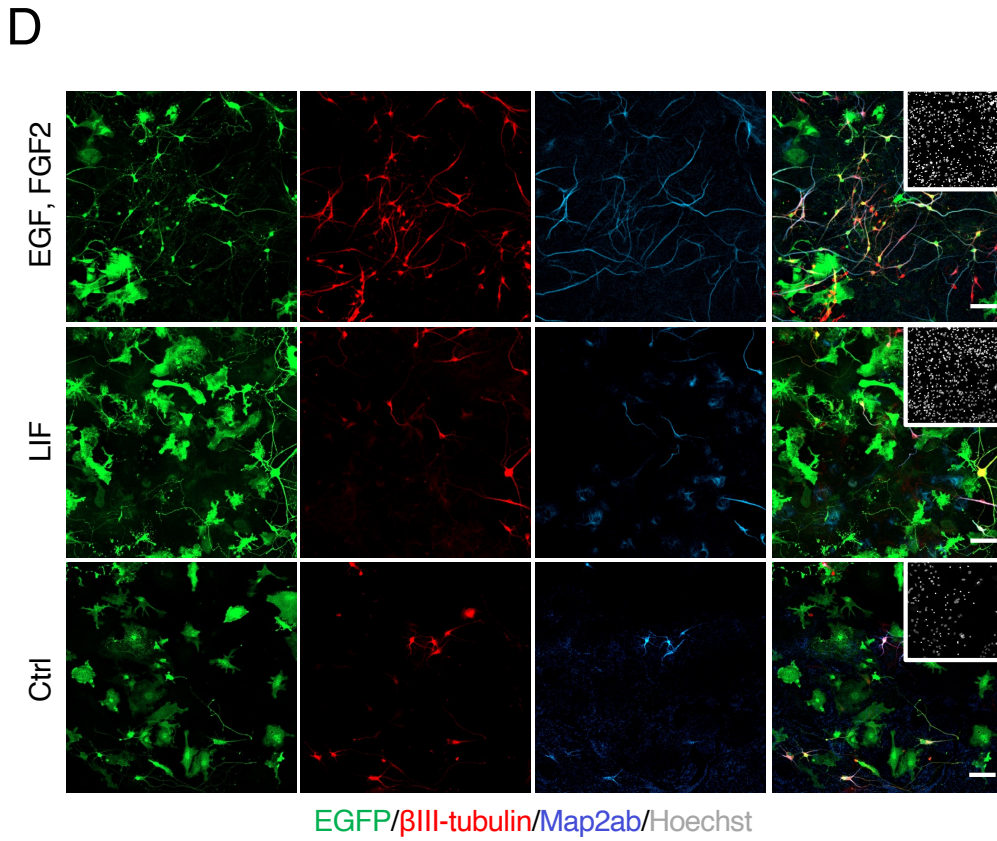
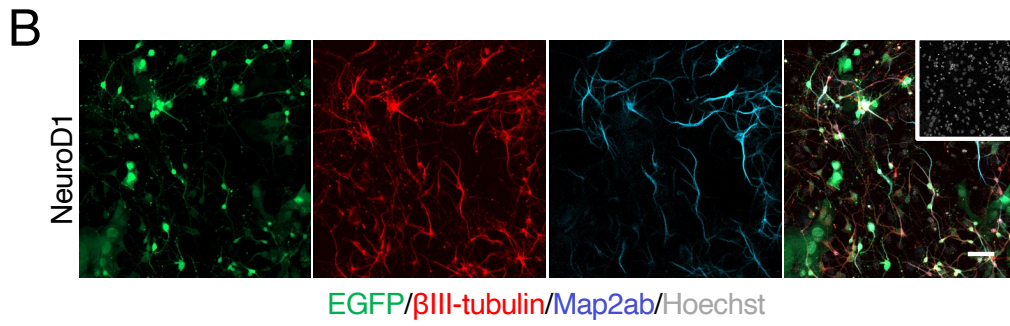
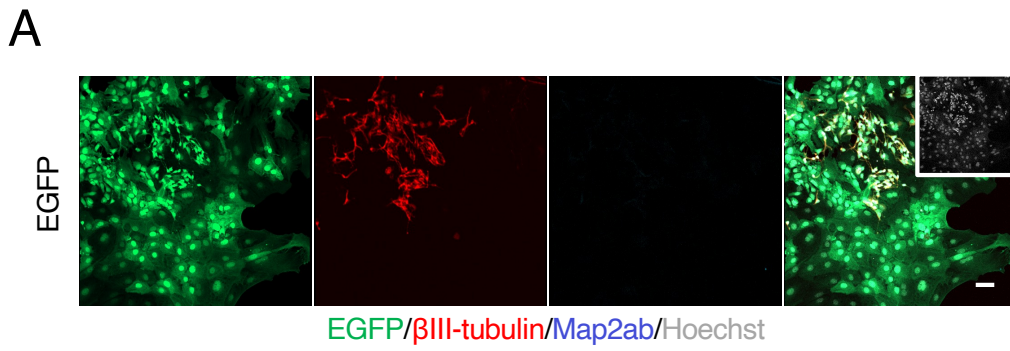


Fig. 3

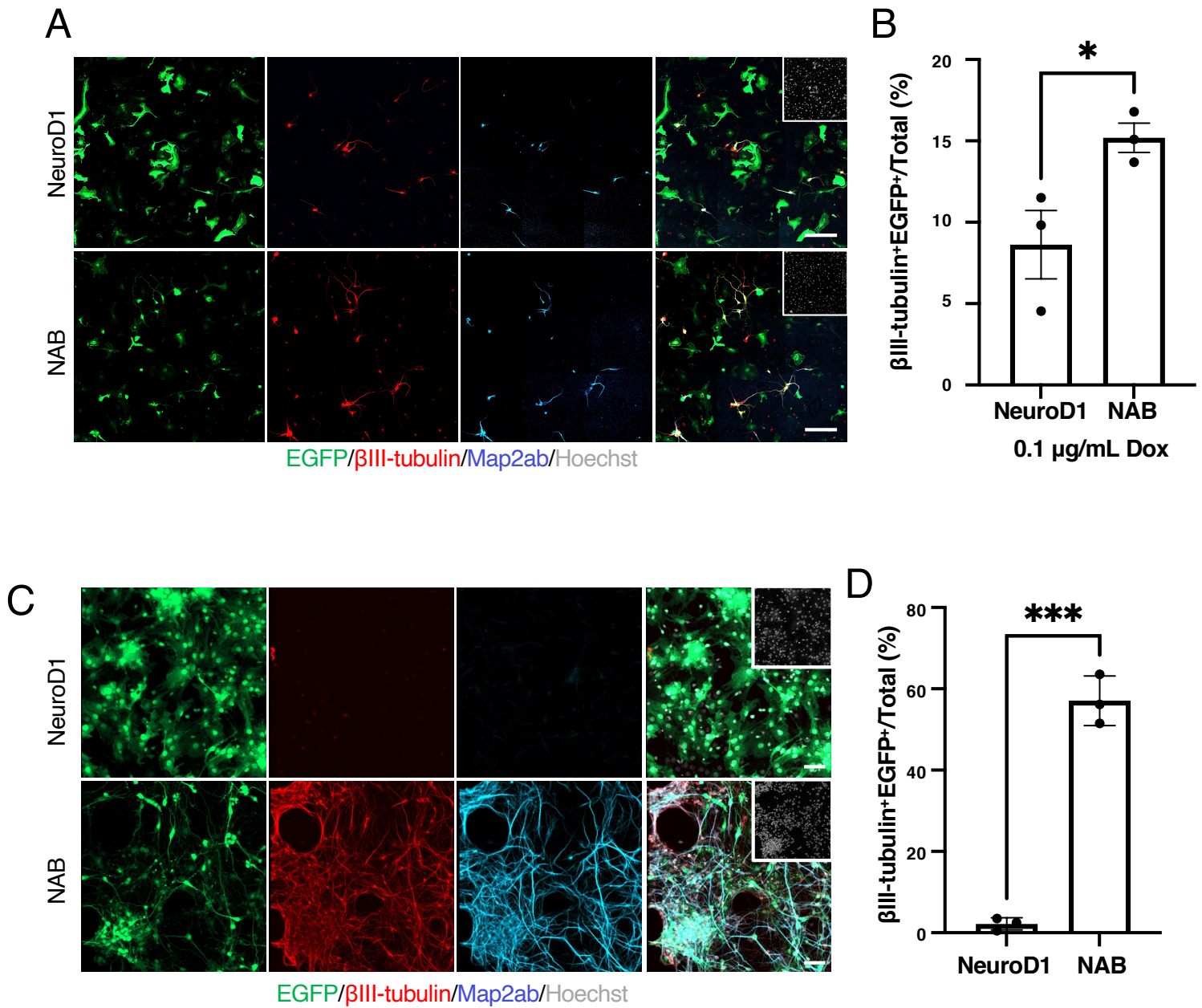


Fig. 4